From Thermal to Electroactive Graphene Nanofluids [†]

Daniel Rueda-García [iD]**, María del Rocío Rodríguez-Laguna** [iD]**, Emigdio Chávez-Angel** [iD]**,**
Deepak P. Dubal, Zahilia Cabán-Huertas, Raúl Benages-Vilau and Pedro Gómez-Romero *

Catalan Institute of Nanoscience and Nanotechnology, ICN2 (CSIC-BIST), Campus de la UAB,
08193 Bellaterra (Barcelona), Spain; ruedizzi@gmail.com (D.R.-G.); rodriguez3laguna@gmail.com (M.d.R.L.);
emigdio.chavez@icn2.cat (E.C.-A.); dubaldeepak2@gmail.com (D.P.D.); hazalia@gmail.com (Z.C.-H.);
raul.benages@icn2.cat (R.B.-V.)
* Correspondence: pedro.gomez@icn2.cat
† This paper is an extended version of our paper published in ICNf2019. 1st International Conference on
Nanofluids, Castellón, Spain, 26–28 June 2019.

check for updates

Abstract: Here, we describe selected work on the development and study of nanofluids based on graphene and reduced graphene oxide both in aqueous and organic electrolytes. A thorough study of thermal properties of graphene in amide organic solvents (N,N-dimethylformamide, N,N-dimethylacetamide, and N-methyl-2-pyrrolidone) showed a substantial increase of thermal conductivity and specific heat upon graphene integration in those solvents. In addition to these thermal studies, our group has also pioneered a distinct line of work on electroactive nanofluids for energy storage. In this case, reduced graphene oxide (rGO) nanofluids in aqueous electrolytes were studied and characterized by cyclic voltammetry and charge-discharge cycles (i.e., in new flow cells). In addition, hybrid configurations (both hybrid nanofluid materials and hybrid cells combining faradaic and capacitive activities) were studied and are summarized here.

Keywords: graphene; reduced graphene oxide (rGO); nanofluids; thermal properties; heat transfer fluids; electrochemical energy storage; electroactive nanofluids

---

1. Introduction

An increasing number of applications related to energy conversion and storage rely on graphene because of its extraordinary combination of properties [1,2]. Graphene is a solid material and it has been used as such in all these applications, however, fluids are strategic materials used in a wide range of industrial applications, which span from thermal to biomedical or to electrochemical systems. In particular, nanofluids, which integrate solid nanoparticles dispersed in a base liquid and constitute a new type of materials with ground-breaking new properties, provide new opportunities to advance in many fields. Heat transfer is currently the most intensively explored application. However, magnetic ferrofluids, health applications, and energy storage appear as other promising fields of study and potential application [3,4].

The nature of the solid phases used in the preparation of nanofluids is extremely varied. In the case of heat transfer fluids (HTFs), all types of solids, from metals to oxides to carbons have been widely studied given the superior thermal conductivity of solids as compared to liquids [5], however, magnetic or electrochemical nanofluids are much more restricted to phases with the necessary magnetic or electroactive nature. In the latter type, electroactivity can be redox [6,7] or capacitive [8], although hybrid materials and devices combining both of those are also possible [9]. In electroactive nanofluids, nanoparticles are dispersed into a base fluid that must be an ionic-conducting electrolyte. This represents an additional challenge in order to avoid coagulation processes which are frequently associated with the presence of ionic salts in the medium.

Electroactive nanofluids can be used in flow cells. These are a special type of energy storage system in which electroactive fluids are stored out of the electrochemical cell and are forced to circulate through it by pumping. This configuration leads to the decoupling of energy density (which is determined by the volume of the external tanks) and power (which will depend on the active area of the cell electrodes). This has led to the development of modular designs that are best suited for stationary energy storage, but able to meet any requirement, and therefore are a perfect solution to be coupled with intermittent power generation similar to that associated with renewable energies.

Graphene nanofluids are prepared by dispersing graphene (or RGO) nanosheets in an adequate base fluid. They can be stabilized in organic or aqueous solvents [6,8,10,11] in the form of pure, non-oxidized graphene [11] or rGO [8], but also in the form of hybrids [6,10]. All of these solvents present useful thermal or electrochemical properties, among others, as we summarize below. Indeed, this study is an extended overview of our recent work on functional nanofluids with an emphasis on their thermal and especially on their electrochemical properties and applications, as presented at the 1st International Conference of Nanofluids [12].

2. Materials and Methods

Graphene flakes with lateral sizes ~150–450 nm and thicknesses from 1 to 10 layers were prepared from graphite (Sigma-Aldrich, purity >99% and size <20 μm) by a mechanical exfoliation method, as described in a previous work [11].

Graphene oxide (GO) was synthesized from graphite using a modified Hummers method. Briefly, 5 g $NaNO_3$ and 225 ml H_2SO_4 were added to 5 g graphite and stirred for 30 min in an ice bath. Then, 25 g $KMnO_4$ was added to the resulting solution, and the solution was stirred at 50 °C for 2 h. Then, 500 ml deionized water and 30 ml H_2O_2 (35%) were slowly added to the solution, and the solution was washed with dilute HCl. Next, the GO product was washed again with 500 ml concentrated HCl (37%). The reduced graphene oxide was prepared by high temperature treatment of the GO sample at 800 °C.

In the second step, we prepared hybrid materials based on rGO, phosphomolybdic acid (rGO-PMo_{12}, where PMo_{12} is the short notation for $H_3PMo_{12}O_{40}$) and phosphotungstic acid (rGO-PW_{12}, where PW_{12} is the abbreviation for $H_3PW_{12}O_{40}$). Briefly, 0.25 g of rGO was dispersed in 100 ml of deionized water with a probe sonicator (of power 1500 watt) for 1 h. Then, 10 mM of the corresponding POM was added to the presonicated rGO dispersion. This suspension was further sonicated (ultrasonic bath 200 watt) for 5 h and kept at room temperature for 24 h. Afterwards, the product was filtered off and dried in a vacuum oven at 80 °C, overnight.

Electroactive nanofluids were prepared by direct mixing of rGO with the base fluid. In this study, the base fluid is distilled water 1 M H_2SO_4. Nanofluids with different concentrations were prepared by mixing 0.025, 0.1, and 0.4 wt% of rGO in 1 M H_2SO_4 aqueous solution. In order to get a stable dispersion, 0.5 wt% of surfactant (triton X-100) was added and the mixture was kept in an ultrasonic bath for up to 2 h.

Thermal conductivity was measured using a modified three-omega (3ω) method based on the work of Oh et al. [13]. Finally, the stability of the dispersions was studied over time by regular tests every month for four months using dynamic light scattering (DLS) with a ZetaSizer nano ZS (ZEN3600, Malvern Instruments, Ltd., Malvern, UK). The rheological measurements were carried out with a rheometer (HAAKE RheoStress RS600, Thermo Electron Corporation). Electrochemical characterizations such as cyclic voltammetry (CV), galvanostatic charge/discharge (chronopotentiometry, CP), chronoamperometry (CA), and electrochemical impedance measurements of rGO nanofluid symmetric cell were carried out with Biologic SP200 and VMP3 potentiostats.

3. Thermal Graphene Nanofluids

We have designed and prepared stable graphene nanofluids for thermal applications. Several organic solvents were used, in particular N,N-dimethylformamide (DMF),

N,N-dimethylacetamide (DMAc), and N-methyl-2-pyrrolidone (NMP). Thermal conductivity data can be found in Figure 1, which allows comparison of pure DMAc and graphene nanofluids in DMAc (0.09 wt% and 0.18 wt%). A 3-ω method adapted to liquid samples was used to carry out the measurements [11]. Specific heat, thermal conductivity and sound velocity were all found to increase with the content of graphene [11]. Thus, a nanofluid with just 0.18 wt% of graphene yielded an enhancement of 48% in thermal conductivity as compared with the solvent, exemplifying how a very small amount of graphene leads to a very substantial effect.
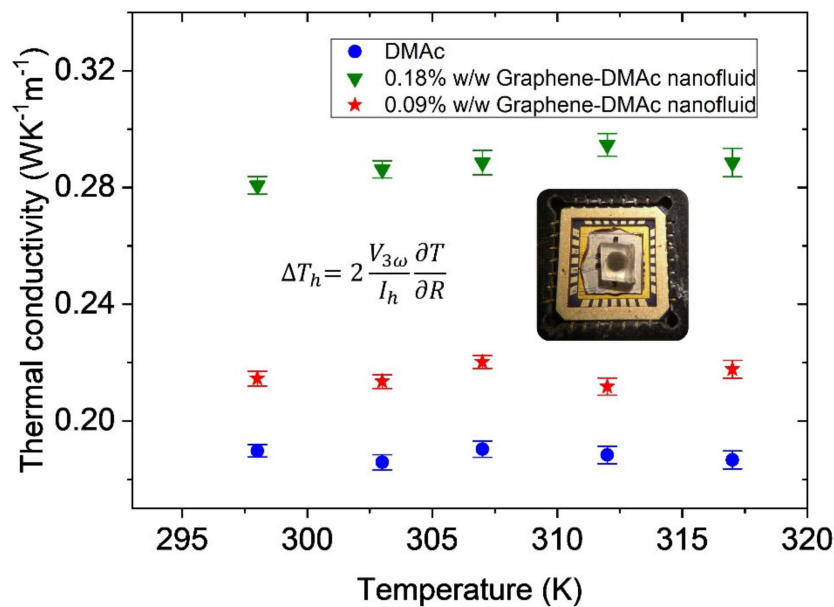

Figure 1. Thermal conductivity as a function of temperature measured through the 3-omega technique for graphene nanofluids in dimethylacetamide solvent.

In order to compare this large effect with theory, we calculated the predicted thermal conductivity enhancement given by effective medium theory (EMT) using the Maxwell equation, given by:

$$\frac{\kappa_m}{\kappa_f} = \frac{\left(2\phi\left(\kappa_p - \kappa_f\right) + 2\kappa_f + \kappa_p\right)}{\left(-\phi\left(\kappa_p - \kappa_f\right) + 2\kappa_f + \kappa_p\right)} \tag{1}$$

where κ_m, κ_f, and κ_p are the thermal conductivities of the effective medium (i.e., nanofluid), base fluid, and nanoparticles, respectively, and ϕ is the particle volume fraction.

If we consider that the $\kappa_f << \kappa_p$ (for DMAc and DMF $\kappa_f = 0.175$ and $0.180\,\text{W K}^{-1}\,\text{m}^{-1}$, respectively, while for graphene $300 < \kappa_p < 3000\,\text{W K}^{-1}\,\text{m}^{-1}$ in the limit of small particle concentrations, Equation (1) is rewritten as:

$$\frac{\kappa_m}{\kappa_f} \cong \frac{(1 + 2\phi)}{(1 - \phi)} \approx (1 + 2\phi)(1 + \phi) \approx 1 + 3\phi \tag{2}$$

Figure 2 (left) shows the comparison using EMT model using Maxwell equation, Equation (1), and a thermal conductivity value of nanoparticles of $kp = 600\,\text{W K}^{-1}\,\text{m}^{-1}$ and its approximation, Equation (2). It can be observed that for very low concentration values both Equations (1) and (2) do not match our experimental observations. Even for a very large span of kp (Figure 2, right) the enhancement predicted by Equation (1) is negligible.

The very poor matching can be related to the assumptions made within the Maxwell model, which only takes into account thermal conductivities of the base fluid and particles and volume fraction of particles, while particle size, shape, and the distribution and motion of dispersed particles, which are not taken into consideration in this model, may have an unaccounted impact on thermal

conductivity enhancement. Therefore, the experimental results could not be compared with the correlated values of this theoretical framework.
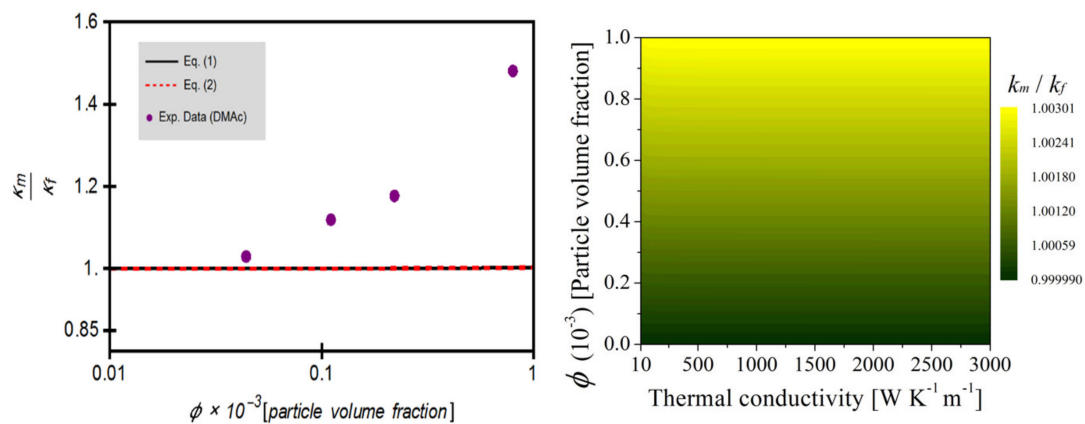

Figure 2. Left: Maxwell equation (Equation (1)) and its approximation (Equation (2)) compared with our measured data. **Right**: Counterplot of Maxwell equation as a function of volume fraction and *kp*.

In this context, a number of works have been published showing different expressions for the effective thermal conductivity of the nanofluids [14]. The modifications to the classical EMT have been mainly associated to the following: particle size, shape, volume fraction, temperature, agglomeration, percolation, nanolayering, and static and dynamic conditions of nanoparticles (Brownian motion and localized convection). Among this sea of theoretical models, one widely used for graphene flakes and nanowires is the so-called Nan's model [15]. According to Nan's model, the thermal conductivity of the nanofluid can be calculated as follows:

$$\frac{\kappa_m}{\kappa_f} = \frac{\phi \left(2\beta_{11} \left(1 - L_{11} \right) + \beta_{33} \left(1 - L_{33} \right) \right) + 3}{\left(3 - \phi \left(2\beta_{11} L_{11} + \beta_{33} L_{33} \right) \right)} \tag{3}$$

$$\beta_{ii} = \frac{\kappa_p - \kappa_f}{L_{ii} \left(\kappa_p - \kappa_f \right) + \kappa_f} \tag{4}$$

where L_{ii} is a form factor which depends on the geometry of the nanoparticle. For the case of graphene flakes, the aspect ratio is very high, and therefore $L_{11} = 0$ and $L_{33} = 1$ [16]. Figure 3 compares Nan's model calculations with our experimental data showing a much better correlation with this model.
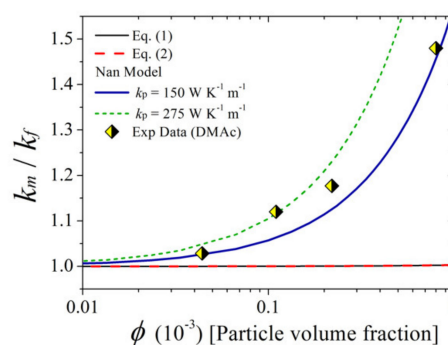

Figure 3. Nan's model and its comparison with our measured data.

In addition to the described trend of thermal conductivity enhancement in graphene nanofluids, we detected a very interesting correlation of this effect (for DMF and DMAc nanofluids) with an overall shift of specific Raman bands in the series of nanofluids (see Figure 4). No band splitting is observed. Instead, the whole bands are broadened and clearly shifted to higher frequencies, with the shift being

proportional to the concentration of graphene. This observation implies that the effect of adding graphene affects the bulk solvent. It should be noted that this shift only takes place for solvents in which the thermal conductivity is increased by graphene, in our case DMF and DMAc, whereas for NMP nanofluids neither a significant thermal conductivity enhancement nor Raman shifts were observed [17]. Possible mechanisms explaining this behavior have been proposed and analyzed elsewhere [11,17].
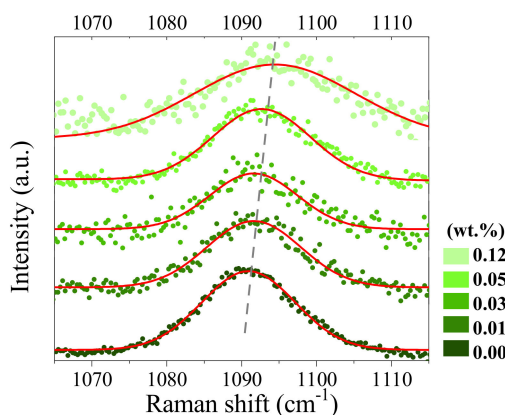

Figure 4. Raman spectra of pure N,N-dimethylformamide (DMF) (**bottom**) and graphene nanofluids with increasing concentrations showing the shift and broadening of the rocking mode peak ascribed to the "(CH3)N" bond in DMF (from ref [11]).

4. Electroactive Graphene Nanofluids

In the area of electrochemical energy storage, our group has pioneered the design and study of electroactive graphene nanofluids. In this case, rGO (prepared by Hummers method, then thermally reduced at 800 °C) was dispersed in acidic aqueous electrolytes and we were able to demonstrate a very fast charge transfer [8,10]. Thus, a dispersion of rGO in 1M H_2SO_4 stabilized in aqueous solution with the addition of a surfactant (0.5 wt% of triton X-100 and sonicated by ultrasonic bath up to 2 h), featured low viscosity values, close to those of water (in the shear rate range of 25 to 150 per s at room temperature). Dispersions of graphene in organic solvents, as the ones described for thermal nanofluids, could also be used for the development of electroactive nanofluids, provided a suitable salt could be dissolved to form the necessary electrolytic solution. Organic solvents would be best suited for (non-oxidized) graphene materials, whereas aqueous electrolytes are perfect to disperse GO or rGO. In our case, preliminary tests, with the addition of various salts to pure graphene in organic solvents, led to dispersions which were less stable in time than those of rGO in dilute sulfuric acid, which is why we proceeded with the latter as a case study for electroactive nanofluids. The specific capacity of this dispersion was similar to that found for solid electrodes in conventional rGO supercapacitors (169 F/g(rGO)). Remarkably, these nanofluids were able to work at faster rates, up to 10,000 mV/s, in 0.025, 0.1, and 0.4 wt% rGO (Figure 5). This fast response confirms the great potential of these nanofluid materials for applications in novel devices which we could call flowing supercapacitors. We should note that even very dilute nanofluids led to full utilization of the dispersed active material.

This effective charge-transfer capacity was corroborated by studying the nanofluid performance under continuous flow conditions. Under flowing conditions, the CVs show identical profiles and they remain identical as flow rates are changed (Figure 6, LEFT). Moreover, we found that the specific capacitance improves under flow conditions (Figure 6 RIGHT) in contrast to semisolid viscous slurries, for which the conductivity, and therefore the capacitance, decrease notably under flow conditions [18]. We found the maximum capacitance at a flow rate of 10 ml/min in our homemade serpentine flow channel cell.
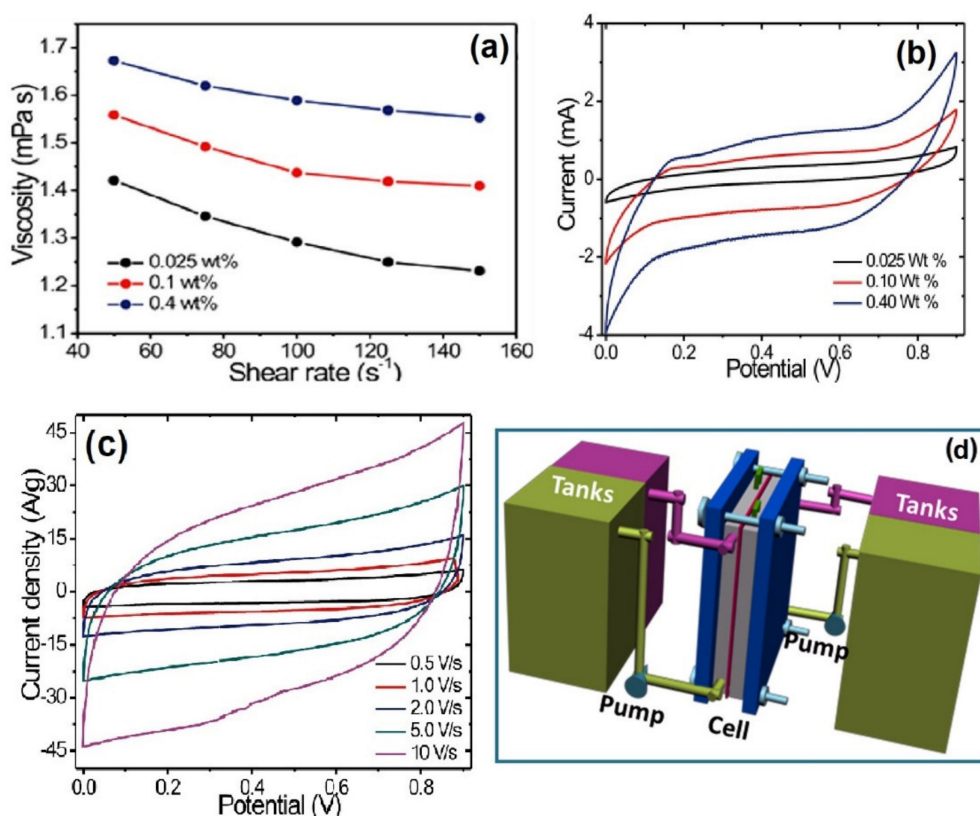
Figure 5. (**a**) Rheological properties of the three nanofluids studied showing low viscosity suitable for efficient pumping, cyclic voltammetry (CV) curves of (**b**) rGO nanofluids of different concentration at 20 mV/s scan rate in static condition and (**c**) rGO nanofluid of 0.025 wt% concentration at different scan rates (data from ref. [8]) (**d**) scheme of the electrochemical system used.
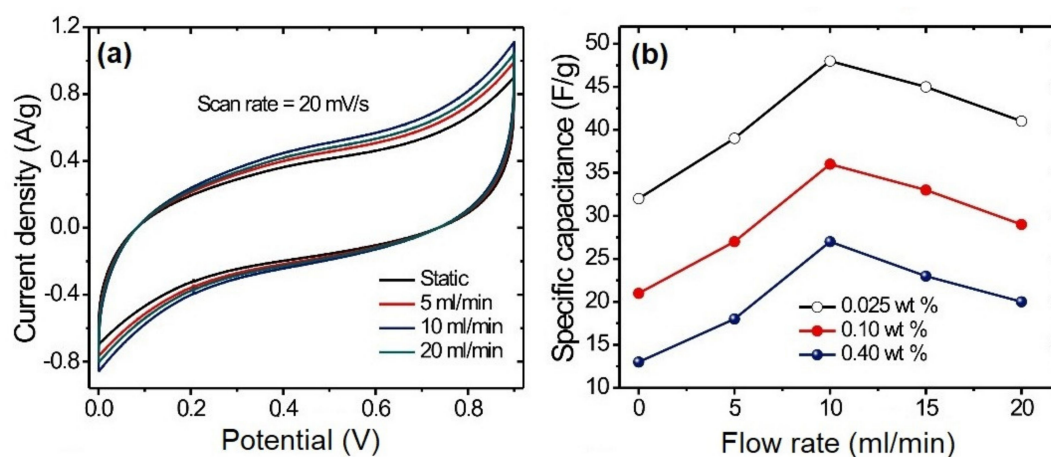

Figure 6. LEFT: CVs (20 mV/s) of 0.025 wt% rGO nanofluids at various flow rates. **RIGHT**: Specific capacitance of varios rGO nanofluids as a function of flow rate (data from ref. [8]).

Concerning the viscosity of our nanofluids, we tried to compare our experimental results with theoretical models (Einstein-Batchelor) but the results showed a poor agreement between our data and the model. However, this is not too surprising given the strong assumptions made in that model, especially the spherical nature of the nanoparticle modeled as compared with the strongly anisotropic nature of graphene nanosheets.

We have also studied nanofluids based on hybrids which in turn were made combining graphene as a conductive and capacitive material with redox-active inorganic species. Thus, some of the

hybrid electroactive nanofluids (HENFs) that we have prepared integrate faradaic and capacitive storage mechanisms simultaneously in a nanofluid. Specifically, we have designed and prepared "liquid electrodes" based on a stable nanocomposite of rGO and polyoxometalates (POMs) and have studied them in a novel flow cell that differs from conventional ones precisely in the use of nanofluids. Two rGO nanocomposites were prepared and a surfactant was used to disperse them in 1M H_2SO_4. The hybrids used two different polyoxometalates (POMs), phosphomolybdic acid (rGO-PMo$_{12}$) and phosphotungstic acid (rGO-PW$_{12}$), which were synthesized by mixing rGO with a solution of the corresponding POM as previously reported [19].

We used a homemade flow cell system (carved serpentine flow 200 mm long path, 5 mm wide, and 1mm in depth, with total cell size of 7 cm × 6 cm × 1 cm) to study these hybrid electroactive nanofluids (HENFs) both under flowing and static conditions [10]. Both nanofluids showed a viscosity very close to that of water (Figure 7a). It should be pointed out that even at low concentrations of rGO-POM (0.025 wt%) high values of specific capacitance were measured for rGO-PW$_{12}$ (273 F/g) and for rGO-PMo$_{12}$ (305 F/g) leading to high specific energy and power densities (Figure 7). Furthermore, after 2000 cycles a good coulombic efficiency (~77% to 79%) was reached and an excellent cycling stability (~95%). According to these results, our POM HENFs act as genuine liquid electrodes and feature outstanding properties. This supports the potential application of this type of HENFs for energy storage applications in nanofluids flow cells.
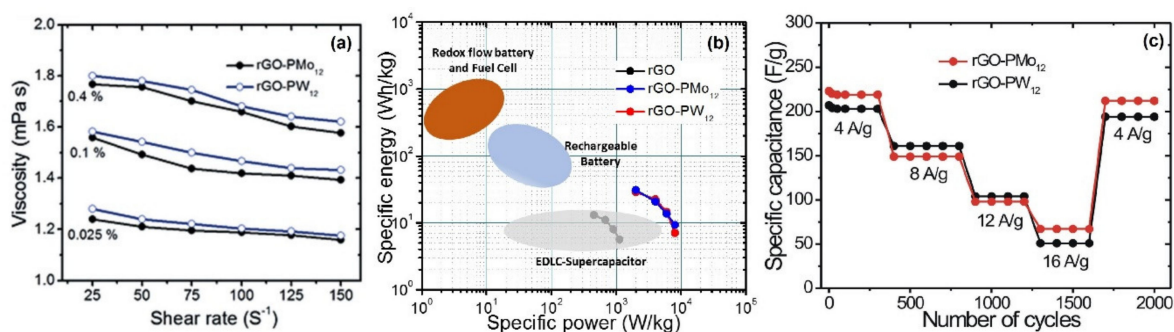

Figure 7. (**a**) The viscosity of rGO, rGO-PMo12 and rGO-PW12 HENFs of different concentrations with shear rate. (**b**) Ragone plot for rGO, rGO-PW12 and rGO-PMo12 nanofluids described in this paper and comparison with other energy storage technologies [9,20–23]. (c) Galvanostatic cycling performance for rGO-POMs hybrid electroactive nanofluids of 0.025% at various current densities for 2000 cycles (data from ref [10]).

It should be underscored that we were able to fully utilize the dispersed rGO nanosheets. Both our energy and power density values are even slightly better (6 to 30 Wh kg−1$_{rGO-POM}$ and 2 to 9 kW kg−1$_{rGO-POM}$) than those reported in the literature for the corresponding solid electrodes [24]. On the one hand, it should also be noted that in our case only a small fraction of the fluid mass is electroactive (in contrast with conventional solid electrodes). Indeed, increasing the load of active material is the most important remaining challenge for these novel electroactive nanofluids. A greater concentration of electroactive rGO or a greater concentration of POM in rGO-POM would lead to a proportionally greater capability to store electrons per unit volume of bulk fluid. On the other hand, both aqueous reduced graphene nanofluids showed limited stability. Ten hours after dispersion a change in the opacity of the nanofluids could be appreciated due to the precipitation of rGO, and after 40 hours almost all the rGO had precipitated.

We developed a new kind of aqueous nanofluid as proof of concept to obtain a solution with increased stability of the rGO without using any surfactant and at the same time keeping the fast charge transfer capability and low viscosity. Thus, in order to improve the stability of rGO, we dissolved an aromatic molecule in the dispersion with the potential to establish π–π interactions with rGO, avoiding or at least hindering its restacking and precipitation, but at the same time leaving free the edges to transfer the charge between rGO layers without increasing the viscosity. We used 3,4-diaminobenzoic

acid (DABA) as the dissolved aromatic molecule to stabilize rGO. We found that with a 40:1 mass ratio of DABA to rGO (0.3g/L) the nanofluid is stable up to 97 h instead of 10 h, which is a very substantial improvement [6]. This nanofluid also had LiOH to adjust the pH to seven to ensure good solubility of DABA and as electrolyte salt.

$LiFePO_4$ was chosen as a typical battery material to test the charge transfer capacity of our DABA-stabilized rGO nanofluid. Thus, various amounts of $LiFePO_4$ nanoparticles were added to the DABA/rGO nanofluid. On the one hand, it should be noted that neither rGO alone, nor $LiFePO_4$ nanoparticles alone (both dispersed in the same $LiOH/1M$ Li_2SO_4 electrolyte), showed any redox response (Figure 8).

On the other hand, $LiFePO_4$ nanoparticles dispersed in the DABA/rGO nanofluid showed the characteristic redox peaks corresponding to Li+ de- and intercalation in $LiFePO_4$. These redox peaks were clearly observed even at fast scan rates (for an intercalation material) of 25 mV/s (Figure 9), indeed, we were able to detect the redox peaks at 100mV/s, but above 25 mV/s the separation between them increased, implying an excessive resistance at those scan rates.
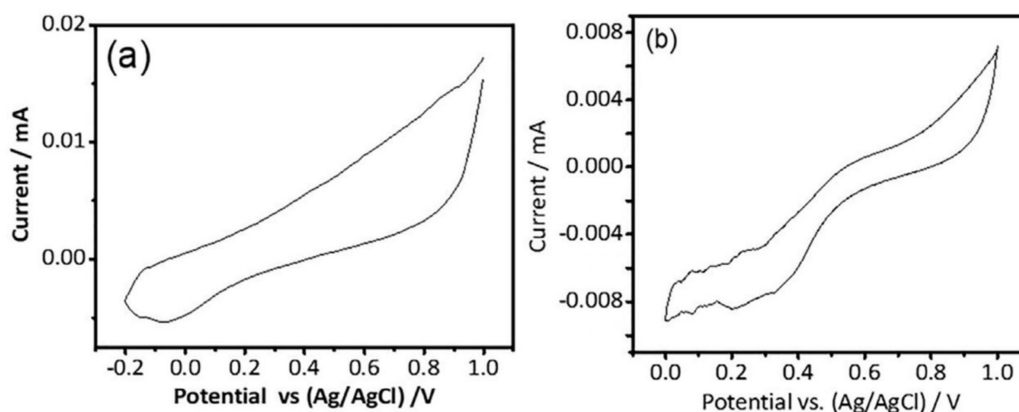

Figure 8. CVs of (**a**) reduced graphene oxide (rGO) and (**b**) $LiFePO_4$ (1.4 g/L) in water electrolyte (scan rate 5 mV/s). (Reprinted with permission from Rueda-García, Daniel et al. This article was published in Electrochemica Acta, 281, 598 (2018), copyright 2018 Elsevier.)
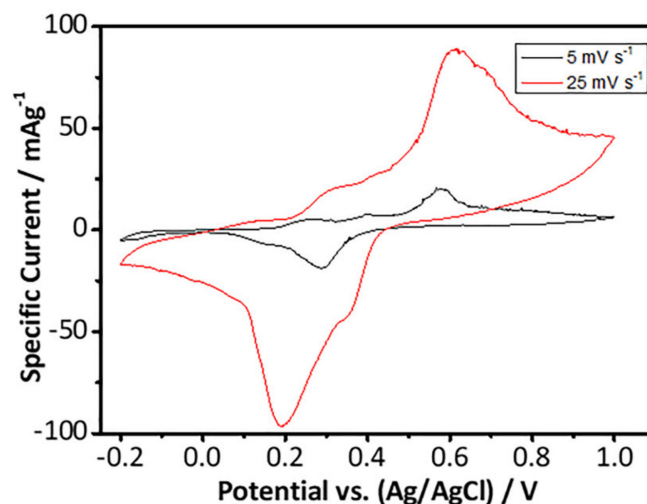

Figure 9. CV of faradaic $LiFePO_4$ (1 g/L) with capacitive3,4-diaminobenzoic acid reduced graphene oxide (DABA/rGO) (40:1). (Reprinted with permission from Rueda-García, Daniel et al. This article was published in Electrochemica Acta, 281, 598 (2018), copyright 2018 Elsevier.)

The detection of $LiFePO_4$ redox peaks only in the presence of rGO proves that rGO provides the electrons needed for the redox process of the $LiFePO_4$ nanoparticles in an effective way that the

inorganic nanoparticles could not get by themselves due to their sluggish diffusion in the current collectors. Moreover, we were also able to fully charge and discharge the LiFePO$_4$ nanoparticles dispersed with high coulombic efficiency which proves that rGO provides charge to the total volume of the nanofluid, thus, leading to a full charge and discharge of the bulk material in the nanofluid.

5. Summary and Conclusions

Notwithstanding the importance of nanofluids for thermal energy transfer and storage, which we have also studied, we have shown in this article the potential of nanofluids in other novel applications, namely, electrochemical energy storage. From the results shown here, we can induce important general conclusions concerning the extended effects of small amounts of solid (in our case graphene) throughout the whole volume of the nanofluid. These effects are present both in thermal, as well as in electrochemical systems. Thus, thermal conductivity is notably enhanced (48%) by a tiny amount of graphene (0.18%) because, surprisingly, this tiny amount of graphene affects the bulk of the solvent molecules. Furthermore, other properties such as specific heat and sound velocity also change remarkable, and we have been able to show a correlation between the enhancement of these thermal properties and the Raman spectra of the bulk fluids.

Nevertheless, we have proven that stable rGO water dispersions are able to transfer charge through all the nanofluid volume, which lead to the whole nanofluid acting as a supercapacitor electrode storing charge through a capacitive mechanism. Indeed, the rGO aqueous nanofluid showed an extremely fast charge transfer, capable of cycling at 10V/s. Thanks to this fast charge transfer we were able to completely charge, and discharge, dispersed redox active nanoparticles of LiFePO$_4$ and clearly detect its redox waves even at 25 mV/s. Moreover, doping the rGO with molecular active redox species, such as the polyoxometalates, we developed hybrid systems with improved power and capacity with respect to the pure rGO nanofluid.

Finally, we have shown the outstanding stability of graphene nanofluids in amide solvents (DMF, DMAc, and NMP) in the absence of any surfactant and have shown how to stabilize rGO in aqueous saline electrolytes (we proved that aqueous rGO nanofluids can improve their stability by dissolving an aromatic molecule (DABA) able to stabilize rGO by π–π interactions while keeping its good electrical conductivity). All of this has been possible maintaining the viscosity of the nanofluids developed very close to that of the parent solvents, which will facilitate their final application in real flowing devices. However, the low concentration of graphene nanosheets could be a handicap for the application of these materials in high-energy density devices. Therefore, an important goal is increasing the loading of electroactive nanoparticles. Other pioneering groups, for example, Timofeeva et al. have been able to show that it is possible to develop electroactive nanofluids which can maintain low viscosity and high loading of electroactive nanoparticles (surface-modified TiO$_2$ in their case) [7,25], thus, showing that this is not an intrinsic barrier for this type of material.

Furthermore, other groups are also contributing to the development of this field, working both with polyoxometalate clusters [26] or oxides (Fe$_2$O$_3$) [27] and exploring new media such as ionic liquids as base fluid for electroactive nanofluids [27].

In summary, we have designed and prepared nanofluids based on graphene but also on graphene hybrids, both in aqueous and organic electrolytes. We have shown how these novel nanofluid materials can feature outstanding performances even in the case of very dilute systems. Both, in the case of thermal properties as well as when it comes to electrochemical properties, we have demonstrated nonlinear effects, leading to remarkable properties with small amounts of graphene dispersed in the nanofluids. Thus, our work underscores the solid potential of these systems as heat transfer fluids and energy storage applications, respectively.

Author Contributions: Conceptualization, D.R.-G. and P.G.-R.; data curation, E.C.-A.; investigation, D.R.-G., M.d.R.R.-L., E.C.-A., D.P.D., R.B.-V. and Z.C.-H.; methodology, D.R.-G., M.d.R.R.-L., E.C.-A., and D.P.D.; project administration, R.B.-V.; supervision, P.G.-R.; writing—original draft, D.R.-G.; writing—review and editing, P.G.-R.

Conflicts of Interest: The authors declare no conflict of interest.

References

1. Novoselov, K.S.; Fal, V.I.; Colombo, L.; Gellert, P.R.; Schwab, M.G.; Kim, K. A roadmap for graphene. *Nature* **2012**, *490*, 192–200. [CrossRef] [PubMed]

2. Bonaccorso, F.; Colombo, L.; Yu, G.; Stoller, M.; Tozzini, V.; Ferrari, A.C.; Pellegrini, V. Graphene, related two-dimensional crystals, and hybrid systems for energy conversion and storage. *Science* **2015**, *347*. [CrossRef] [PubMed]

3. Sadeghinezhad, E.; Mehrali, M.; Saidur, R.; Mehrali, M.; Latibari, S.T.; Akhiani, A.R.; Metselaar, H.S.C. A comprehensive review on graphene nanofluids: Recent research, development and applications. *Energy Convers. Manag.* **2016**, *111*, 466–487. [CrossRef]

4. Taylor, R.; Coulombe, S.; Otanicar, T.; Phelan, P.; Gunawan, A.; Lv, W.; Tyagi, H. Small particles, big impacts: A review of the diverse applications of nanofluids. *J. Appl. Phys.* **2013**, *113*, 1. [CrossRef]

5. Kakaç, S.; Pramuanjaroenkij, A. Review of convective heat transfer enhancement with nanofluids. *Int. J. Heat Mass Transf.* **2009**, *52*, 3187–3196. [CrossRef]

6. Rueda-Garcia, D.; Cabán-Huertas, Z.; Sánchez-Ribot, S.; Marchante, C.; Benages, R.; Dubal, D.P.; Ayyad, O.; Gómez-Romero, P. Battery and supercapacitor materials in flow cells. Electrochemical energy storage in a LiFePO4 / reduced graphene oxide aqueous nano fluid. *Electrochim. Acta* **2018**, *281*, 594–600.

7. Sen, S.; Govindarajan, V.; Pelliccione, C.J.; Wang, J.; Miller, D.J.; Timofeeva, E.V. Surface Modification approach to TiO_2 nanofluids with high particle concentration, low viscosity, and electrochemical activity. *ACS Appl. Mater. Interfaces* **2015**, *7*, 20538–20547. [CrossRef]

8. Dubal, D.P.; Gomez-Romero, P. Electroactive graphene nanofluids for fast energy storage. *2D Mater.* **2016**, *3*, 031004. [CrossRef]

9. Dubal, D.P.; Ayyad, O.; Ruiz, V.; Gómez-Romero, P. Hybrid energy storage: The merging of battery and supercapacitor chemistries. *Chem. Soc. Rev.* **2015**, *44*, 1777–1790. [CrossRef]

10. Dubal, D.P.; Rueda-Garcia, D.; Marchante, C.; Benages, R.; Gomez-Romero, P. Hybrid graphene-polyoxometalates nanofluids as liquid electrodes for dual energy storage in novel flow cells. *Chem. Rec.* **2018**, *18*, 1076–1084. [CrossRef]

11. Rodríguez-Laguna, M.D.R.; Castro-Alvarez, A.; Sledzinska, M.; Maire, J.; Costanzo, F.; Ensing, B.; Chávez-Ángel, E. Mechanisms behind the enhancement of thermal properties of graphene nanofluids. *Nanoscale* **2018**, *10*, 15402–15409. [CrossRef] [PubMed]

12. Hermann, H.; Schubert, T.; Gruner, W.; Mattern, N. Structure and chemical reactivity of ball-milled graphite. *Nanostructured Mater.* **1997**, *8*, 215–229. [CrossRef]

13. Oh, D.W.; Jain, A.; Eaton, J.K.; Goodson, K.E.; Lee, J.S. Thermal conductivity measurement and sedimentation detection of aluminum oxide nanofluids by using the 3ω method. *Int. J. Heat Fluid Flow* **2008**, *29*, 1456–1461. [CrossRef]

14. Azmi, W.H.; Sharma, K.V.; Mamat, R.; Najafi, G.; Mohamad, M.S. The enhancement of effective thermal conductivity and effective dynamic viscosity of nanofluids—A review. *Renew. Sustain. Energy Rev.* **2016**, *53*, 1046–1058. [CrossRef]

15. Nan, C.W.; Shi, Z.; Lin, Y. A simple model for thermal conductivity of carbon nanotube-based composites. *Chem. Phys. Lett.* **2003**, *375*, 666–669. [CrossRef]

16. Mehrali, M.; Sadeghinezhad, E.; Latibari, S.T.; Kazi, S.N.; Mehrali, M.; Zubir, M.N.B.M.; Metselaar, H.S.C. Investigation of thermal conductivity and rheological properties of nanofluids containing graphene nanoplatelets. *Nanoscale Res. Lett.* **2014**, *9*, 15. [CrossRef]

17. Rodríguez-Laguna, M.D.R.; Romero, P.G.; Torres, C.M.S.; Chavez-Angel, E. Modification of the raman spectra in graphene-based nanofluids and its correlation with thermal properties. *Nanomaterials* **2019**, *9*, 804. [CrossRef]

18. Lee, J.; Weingarth, D.; Grobelsek, I.; Presser, V. Use of surfactants for continuous operation of aqueous electrochemical flow capacitors. *Energy Technol.* **2016**, *4*, 75–84. [CrossRef]

19. Dubal, D.P.; Suarez-Guevara, J.; Tonti, D.; Enciso, E.; Gomez-Romero, P. A high voltage solid state symmetric supercapacitor based on graphene-polyoxometalate hybrid electrodes with a hydroquinone doped hybrid gel-electrolyte. *J. Mater. Chem.* **2015**, *3*, 23483–23492. [CrossRef]

20. Ding, Y.; Zhang, C.; Zhang, L.; Zhou, Y.; Yu, G. Molecular engineering of organic electroactive materials for redox flow batteries. *Chem. Soc. Rev.* **2018**, *47*, 69–103. [CrossRef]

21. Chen, R. Toward High-Voltage, Energy-Dense, and durable aqueous organic redox flow batteries: Role of the supporting electrolytes. *ChemElectroChem* **2019**, *6*, 603–612. [CrossRef]

22. González, A.; Goikolea, E.; Barrena, J.A.; Mysyk, R. Review on supercapacitors: Technologies and materials. *Renew. Sustain. Energy Rev.* **2016**, *58*, 1189–1206. [CrossRef]

23. Nitta, N.; Wu, F.; Lee, J.T.; Yushin, G. Li-ion battery materials: Present and future. *Mater. Today* **2015**, *18*, 252–264. [CrossRef]

24. Kamila, S.; Mohanty, B.; Samantara, A.K.; Guha, P.; Ghosh, A.; Jena, B.; Jena, B.K. Highly active 2D layered MoS 2-rGO hybrids for energy conversion and storage applications. *Sci. Rep.* **2017**, *7*, 8378. [CrossRef] [PubMed]

25. Sen, S.; Chow, C.M.; Moazzen, E.; Segre, C.U.; Timofeeva, E.V. Electroactive nanofluids with high solid loading and low viscosity for rechargeable redox flow batteries. *J. Appl. Electrochem.* **2017**, *47*, 593–605. [CrossRef]

26. Friedl, J.; Holland-Cunz, M. V.; Cording, F.; Pfanschilling, F. L.; Wills, C.; McFarlane, W.; Stimming, U. Asymmetric polyoxometalate electrolytes for advanced redox flow batteries. *Energy Environ. Sci.* **2018**, *11*, 3010–3018. [CrossRef]

27. Joseph, A.; Xavier, M.M.; Fal, J.; Żyła, G.; Sasi, S.; Nair, P.R.; Mathew, S. Synthesis and electrochemical characterization of electroactive IoNanofluids with high dielectric constants from hydrated ferrous sulphate. *Chem. Commun.* **2019**, *55*, 83–86. [CrossRef]